Natural convection on one side of a vertical wall embedded in a Brinkman-porous medium coupled with film condensation on the other side

A. Vovos and D. Poulikakos*

A theoretical study of conjugate natural convection and film condensation in porous media is reported. The natural convection phenomenon takes place along one side of a vertical impermeable wall and the condensation phenomenon along the other side. This wall constitutes the interface between two spaces filled with fluid-saturated porous media. The flow in both porous spaces is modelled on the basis of the Brinkman-modified Darcy momentum equation which satisfies the condition of zero velocity on a solid boundary. The temperature and flow fields in the porous medium are completely determined in the natural convection side as well as in the condensation side of the wall. In addition, the dependence of the wall heat flux and temperature distributions on height and on a number of dimensionless groups relevant to the problem is thoroughly documented. Important results pertinent to the impact of the problem parameters on the overall heat leak from the condensation space to the natural convection space are also reported. These results are presented with the help of the Nusselt number. Finally, the effect of the wall thermal resistance on the heat and fluid flow characteristics of the system is determined.

Keywords: *natural convection, film condensation, Brinkman-porous medium, vertical wall*

Introduction

The phenomenon of natural convection, as well as the phenomenon of film condensation along a vertical wall embedded in a porous medium have constituted the focus of a number of investigations in the heat transfer literature[1-7]. Each of the above problems is of fundamental value as well as of practical value in thermal engineering applications in which porous materials play a pivotal role. Some examples of these applications are geothermal systems, grain storage, thermal insulations, oil extraction, and heat and mass transfer through filtering devices.

The present study investigates a case of interaction between the above-mentioned two fundamental problems. More specifically, the configuration of interest is a vertical impermeable wall embedded in porous medium. The porous medium on one side of the wall contains vapour at saturation temperature (T_s). The other side of the wall faces a fluid-saturated porous reservoir at temperature T_c where $T_c < T_s$. It is expected that natural convection along the side of the wall facing the cold reservoir will take place. Similarly, the cooling effect of the natural convection space will initiate condensation along the side of the wall facing the condensation reservoir. The phenomenon described above (also shown schematially in Fig 1) may occur in multilayered fibrous or granular thermal insulations as well as in grain storage applications. With reference to the former, it models the phenomenon in which a vertical layer in a layered insulation system has a moisture content high enough so that condensation is initiated along the boundary separating this layer from its neighbouring layer. With reference to the latter, condensation and natural convection along vertical partitions in storage tanks containing grain is not uncommon. Noncondensible components may be present in the vapour phase in the above applications. Their presence is not taken into account in this study. We are not aware of any experimental studies that indicate that the presence of noncondensible components in the above applications is of paramount importance. In addition, this phenomenon is of geophysical interest for it provides a simple model for the thermal interaction between underground water and steam reservoirs. To be able to predict the heat and fluid flow characteristics of the system of interest, the two heat transfer modes (condensation and natural convection) developing within the two reservoirs sandwiching the wall need to be considered simultaneously for they are coupled through the wall. Unlike the classical problems of natural convection and film condensation from a vertical plate[1-7], where the plate temperature distribution or the plate heat flux distribution is prescribed, the wall temperature distribution and heat flux distribution in the present problem are not known, and they are obtained from the problem solution. This is one of the novel features of the present study.

The importance of coupling in natural convection problems has been recognized by previous investigators both in classical fluids[8-10] and in porous media[11,12]. With reference to porous media flows, Bejan and Anderson have reported theoretical results pertaining to natural convection interaction through the vertical impermeable interface between two porous reservoirs[12] as well as through the interface between a porous and a fluid reservoir[11]. The method of solution used in Refs 11 and 12 is adopted in this study also. To this end, a boundary layer structure is assumed to exist in the near-wall region of the natural convection reservoir, and the condensation phenomenon is assumed tφ be of the filmwire type. The natural convection side is analysed on the basis of the Oseen linearization method[13] and the condensation side on the basis of thin film analysis[14,15]. The results from each side are next matched on the wall to complete the problem solution.

The flow in the porous medium was modelled on the basis of the Brinkman-modified Darcy law[16,17] which accounts for friction due to macroscopic shear stresses and satisfies the no-slip condition on a solid boundary. Therefore, this model appears to be more appropriate for flows near solid boundaries and for flows through high-permeability porous matrixes[16]. It is

* Department of Mechanical Engineering, University of Illinois at Chicago, P.O. Box 4348, Chicago, IL 60680, USA

0142-727X/87/020093-09$3.00

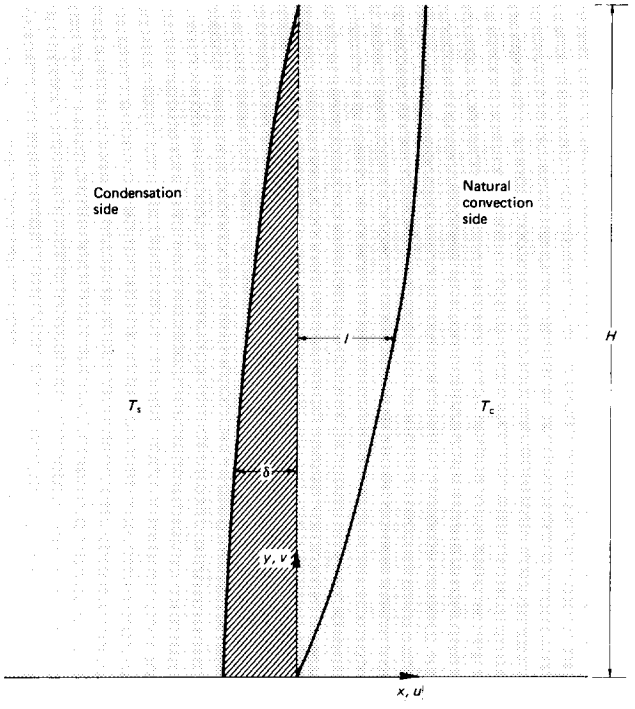

Figure 1 Schematic of the problem of interest. Film condensation in porous medium on the left side of a vertical wall coupled with natural convection in porous medium on the right side of the same wall

worth noting that because of imperfect packing, near-wall regions often exhibit high permeabilities compared with far-wall regions[18,19]. The appropriateness of the Brinkman flow model in natural convection studies has been well established in the literature[4,20-22].

Mathematical formulation

Consider a vertical wall with negligible thermal resistance, separating two fluid-saturated porous reservoirs which remain at different temperatures. The simplifying 'negligible thermal resistance' assumptions, which is equivalent to stating that the wall is thin or of large thermal conductivity or both, will be relaxed at the end of the study. The warmer porous reservoir contains vapour at saturation temperature (T_s) while the colder porous reservoir (T_c) contains a Newtonian fluid.

As discussed in the introduction, the finite temperature difference between the two reservoirs gives life to the conjugate natural convection–condensation heat transfer phenomenon, shown schematically in Fig 1. To formulate the problem mathematically we consider each porous reservoir separately.

Natural convection porous space

According to the Brinkman-modified Darcy model the dimensionless equations, governing the steady-state conservation of mass, momentum and energy in the *boundary layer* are

$$\frac{\partial u}{\partial x}+\frac{\partial v}{\partial y}=0 \tag{1}$$

$$\frac{\partial v}{\partial x}=E\frac{\partial^2 v}{\partial x^3}+\frac{\partial T}{\partial x} \tag{2}$$

$$u\frac{\partial T}{\partial x}+v\frac{\partial T}{\partial y}=\frac{\partial^2 T}{\partial x^2} \tag{3}$$

The dimensionless quantities are defined as follows:

$$x=\frac{x^*}{HRa^{-1/2}},\quad y=\frac{y^*}{H},\quad u=\frac{u^*}{(\alpha/HRa^{-1/2})},$$

$$v=\frac{v^*}{\alpha H^2/(HRa^{-1/2})^2},\quad T=\frac{T^*-\frac{1}{2}(T_s+T_c)}{T_s-T_c} \tag{4}$$

The above nondimensionalization was based on boundary layer scaling[2,20,23,24]. Note that the boundary layer thickness scale ($l\sim HRa^{-1/2}$) was used as the reference length for the horizontal coordinate x^*. Note further that in order to arrive at Eq (2) the pressure gradients in the horizontal and the vertical momentum equations were eliminated and that the Boussinesq approximation was taken into account. According to the

Notation

A Dimensionless group $(k_f Ra^{-1/2})/(kRa_f^{-1/2})$

B Dimensionless group $c_p\dfrac{(T_s-T_c)}{h_{fg}}$

c_p Fluid specific heat at constant pressure
Da Darcy number $\equiv K/H^2$
E Dimensionless group $DaRa$
H Wall height
h_{fg} Latent heat of condensation
K Permeability
k Effective thermal conductivity of porous medium
m Oseen's function
N Dimensionless group $D\alpha^{-1/2}Ra_f^{-1/2}$
Nu Nusselt number
Ra Darcy-modified Rayleigh number based on the wall height $\equiv\dfrac{Kg\beta(T_s-T_c)H}{va}$

Ra_f Film Rayleigh number based on the wall height $\equiv\dfrac{KH(\rho_f-\rho_v)gh_{fg}}{kv(T_s-T_c)}$

L Wall thickness
l Natural convection boundary layer thickness scale
T Temperature
u Horizontal velocity component
v Vertical velocity component
x Dimensionless horizontal Cartesian coordinate
y Dimensionless vertical Cartesian coordinate
w Wall thermal resistance parameter, Eq (24)
α Effective thermal diffusivity of porous medium
β Coefficient of thermal expansion
γ Oseen's function
δ Condensation film thickness
μ Viscosity
ν Kinematic viscosity
ρ Fluid density

Subscripts

c Cold
s Saturation
f Liquid phase in the condensation film
L Left side of the wall
oL Wall temperature, left side
R Right side of the wall
oR Wall temperature, right side
v Vapour phase

Superscripts

* Dimensional quantity, natural convection side
^ Dimensional quantity, condensation side
' Dimensionless quantity, condensation side

Boussinesq approximation the density of the fluid is constant everywhere except in the buoyancy term in the momentum equation, where it depends linearly on the temperature

$$\rho=\rho_\infty\{1-\beta(T^*-T_\infty)\} \tag{5}$$

In Eq (5), β is the coefficient of the thermal expansion of the fluid, and the subscript ∞ denotes a reference state. All the dimensionless groups appearing in this study are defined in the Notation. The boundary conditions for the natural convection side, in porous medium, are

$$\begin{aligned} &x=0: \quad v=0,\ u=0,\ T=T_o(y)\\ &x\to\infty: \quad v=0,\ T=-\tfrac{1}{2}\end{aligned} \tag{6}$$

As mentioned earlier, the wall temperature variation with height in Eq (6) is unknown and it is dictated by the degree of interaction between the two reservoirs.

Condensation porous space

In a recent study, Cheng [6] explains that the governing equations for two-phase flow in porous media are complex due to the fact that a region in the porous medium exists in which the pores are filled partly by liquid and partly by vapour. To account for this fact the concept of relative permeability was introduced, thus rendering the governing equations prohibitively complicated for theoretical solutions. A more tractable mathematical model for two-phase flows in porous media (used in this study) can be obtained on the basis of the following assumptions[6].

(1) A *distinct* boundary exists separating the two phases, ie the vapour and the condensate. This assumption does away with the difficulties associated with the relative permeability: single-phase equations can be applied to describe the flow in the liquid region and the vapour region.
(2) The boundary layer is thin so that the classical thin film analysis can be applied.
(3) The condensate has constant properties.

The model conservation equations for momentum and energy after the above simplifications are

$$\frac{d^2\hat{v}}{d\hat{x}^2}-K^{-1/2}\hat{v}=\frac{\rho_f-\rho_v}{\mu}g \tag{7}$$

$$\frac{d^2\hat{T}}{d\hat{x}^2}=0 \tag{8}$$

The solution for the temperature, the velocity and the film thickness can be obtained by following the procedure used in classical fluids[14,15]. Omitting the details for brevity we present here only the final results in dimensionless form. The intermediate steps are reported in Ref 24.

$$v'=\frac{\cosh K^{-1/2}(\delta'+x')}{\cosh K^{-1/2}\delta'}-1 \tag{9}$$

$$T'=\{T_o(y)-\tfrac{1}{2}\}\frac{x'}{\delta'}+T_o(y) \tag{10}$$

$$\frac{dy'}{d\delta'}=-\delta'\{\operatorname{sech}^2(N\delta')-1\}\times\left\{\frac{1}{\frac{1}{2}-T_o(y)}+B\left[1-\frac{(2-N^2\delta'^2)\cos N\delta'-2}{2N\delta'\cosh(N\delta')\{\tanh(N\delta')-N\delta'\}}\right]\right\} \tag{11}$$

The dimensionless quantities denoted by primes are defined as follows:

$$x'=\frac{\hat{x}}{HRa_f^{-1/2}},\quad \delta'=\frac{\hat{\delta}}{HRa_f^{-1/2}},\quad T'=\frac{\hat{T}-\frac{1}{2}(T_s+T_c)}{T_s-T_c}$$
$$v'=\frac{\hat{v}}{\{(\rho_f-\rho_v)gK/H\}} \tag{12}$$

In order to match the temperature solutions from the two sides of the wall, the wall heat flux continuity condition was used:

$$A\left(\frac{\partial T'}{\partial x'}\right)_{x'=0}=\left(\frac{\partial T}{\partial x}\right)_{x=0} \tag{13}$$

The definition of A (see Notation) implies that the dimensionless group A measures the heat transfer effectiveness of the condensation film relative to the natural convection boundary layer.

Theoretical solution

Expressions for the velocity profile, the temperature profile, and the film thickness in the condensation side are reported in the previous section. In this section, attention is shifted to the natural convection side. For the sake of brevity, no intermediate steps are reported. Details are included in Ref 24. The procedure is similar to that outlined elsewhere[12,20]. The final expressions for the temperature and the velocity fields read

$$v=\frac{T_o+\frac{1}{2}}{2m\gamma E}e^{-mx}\sin\gamma x \tag{14}$$

$$T=\frac{T_o+\frac{1}{2}}{2m\gamma E}\times e^{-mx}[\sin\gamma x-E\{(m^2-\gamma^2)\sin\gamma x-2m\gamma\cos\gamma x\}]-\tfrac{1}{2} \tag{15}$$

where m and γ are unknown functions of y, related via the following equation:

$$\gamma^2=\frac{2m^2E-1}{2E} \tag{16}$$

The problem unknowns are obtained from the simultaneous numerical solution of Eq (11) and the following two equations:

$$\frac{d}{dy}\left\{\frac{(T_o-\frac{1}{2})^3}{(T_o+\frac{1}{2})}\frac{\delta'}{m^2E^2}\left(\frac{1}{m^2}+4E\right)\right\}=64A^2\frac{T_o-\frac{1}{2}}{\delta'} \tag{17}$$

$$A\frac{(T_o-\frac{1}{2})}{(T_o+\frac{1}{2})}=\frac{\delta'}{4mE}(1-4mE) \tag{18}$$

The unknown functions in these three equations are $\delta'(y)$, $m(y)$ and $T_o(y)$. The solution procedure starts with obtaining $m(y)$ from Eq (18) and substituting the result into Eq (17). The resulting expression together with Eq (11) contain two unknowns (δ' and T_o) and they are solved numerically with the help of the Runge–Kutta method. All the details of the numerical solution are contained in Ref 24.

Results and discussion

The main results of the study are presented in this section with the aim of documenting the effect of the dimensionless groups of the problem (A, B, E and N) on the heat and fluid flow characteristics of the conjugate natural convection–condensation phenomenon under investigation. At first, the effect of these groups on the thickness of the condensation film (δ', left side of Fig 2) and the thickness of the natural convection boundary layer ($1/m$, right side of Fig 2) is illustrated. Increasing values of parameter A (solid lines) yield thinner jets on both sides. This effect is more drastic in the condensation side. Parameter B (dashed line) has similar impact on the thickness of the two counterflowing layers; however, the impact of B is significantly weaker. In fact, the effect of B on the natural convection boundary layer thickness is unnoticeable. Decreasing E (dash/dot line) increases the thickness of the condensation film while reducing the thickness of the natural convection boundary layer. Parameter N (long-dash/short-dash line) drastically affects the condensation film; however, its impact on the natural convection boundary layer thickness is

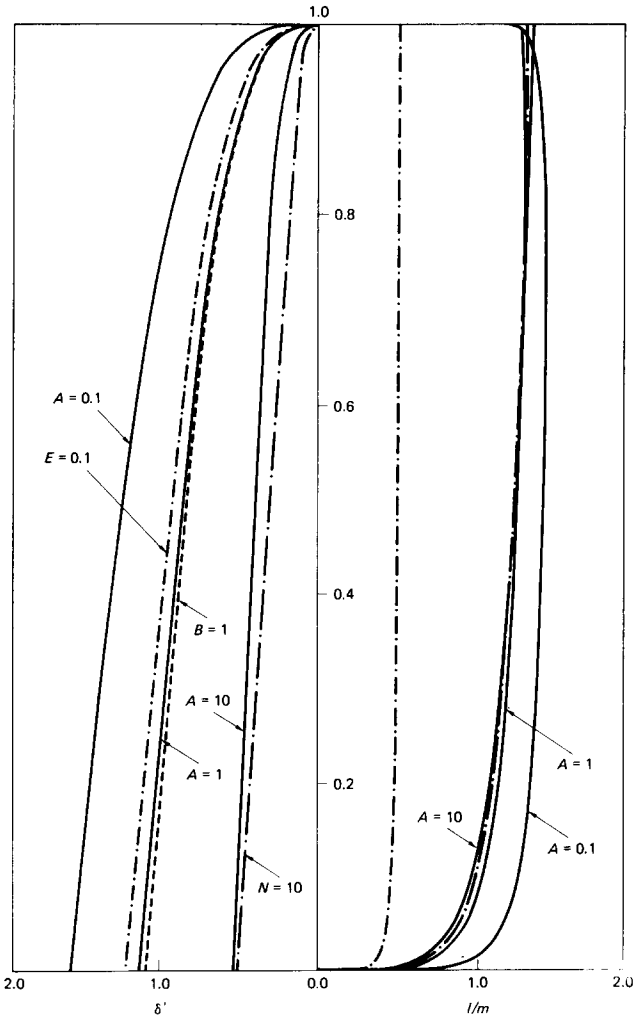

Figure 2 Thickness of the natural convection boundary layer (right) and the condensation film (left) for representative values of *A, B, E, N*. The solid lines are for $B=0.1$ and $N=1$ and depict the effect of *A*. The dashed lines correspond to $A=E=N=1$ and show the effect of *B*. The dash/dot lines are for $A=1$, $B=0.1$, $N=1$ and illustrate the effect of *E*. The long-dash/short-dash lines are for $A=1$, $B=0.1$, $E=1$ and show the effect of *N*

marginal. Fig 2 also illustrates the fact that both the natural convection boundary layer and the condensation film increase in thickness in the flow direction except in the region near $y=1$ where the natural convection boundary layer thickness is reduced to zero. This thickening effect in the flow direction is more noticeable in the condensation side. The line notation used in Fig 2 remains unchanged throughout the study.

Representative results for the velocity and the temperature variations in the two layers at midheight ($y=\frac{1}{2}$) are shown in Figs 3 and 4, respectively. Parameter *A* has a significant effect on both the temperature and the velocity distributions. Increasing *A* increases the temperature drop across the natural convection boundary layer and decreases the temperature drop across the condensation film (Fig 4). As a consequence, increasing values of parameter *A* yield 'fast' natural convection boundary layers and 'slow' films of condensate (Fig 3). The impact of parameter *B* is similar qualitatively to the impact of parameter *A*; however, the dependence of the temperature and velocity distributions on *B* is almost negligible.

Focusing on parameter *E* we see that the effect of decreasing *E* on the temperature distribution is analogous to decreasing parameter *A* (Fig 4). Even though only one value of *E* is shown in Fig 4 this finding was verified for additional values of *E*, less than unity. However, decreasing *E* shifts the velocity maximum closer to the wall (Fig 3). This result makes sense physically since small values of *E* correspond to small values of the Darcy number (if *Ra* is fixed). As *Da* decreases we approach the limit where the Darcy flow model holds[1,11,12,16,20]. In this limit the no-slip condition at the interface is not satisfied and the velocity maximum in the natural convection porous reservoir occurs at the interface. Increasing the last of the parameters, *N*, enhances the temperature difference across the natural convection boundary layer and reduces the temperature difference across the condensation boundary layer (Fig 4). The corresponding impact on the velocity field (Fig 3) resembles that discussed above in conjunction with parameter *A*. The decrease in the temperature drop and the velocity across the film in the condensation side accompanying an increase in *N* is explained by the fact that, if the remaining parameters are fixed, increasing *N* is equivalent to decreasing the film Rayleigh number Ra_f or the porous medium permeability *K* on the condensation side.

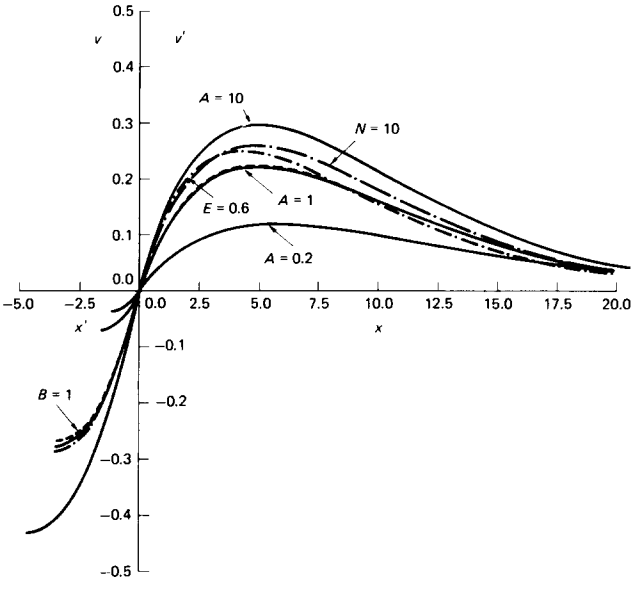

Figure 3 Velocity profiles in the natural convection boundary layer (right) and condensation film (left) at midheight. The notation for the lines is the same as in Fig 2

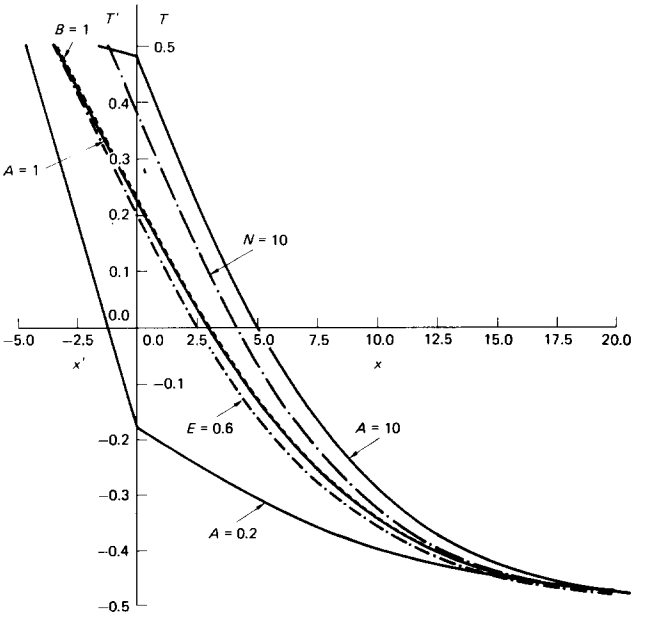

Figure 4 Temperature profiles in the natural convection boundary layer (right) and the condensation film (left) at midheight. The notation for the lines is identical to that used in Fig 2

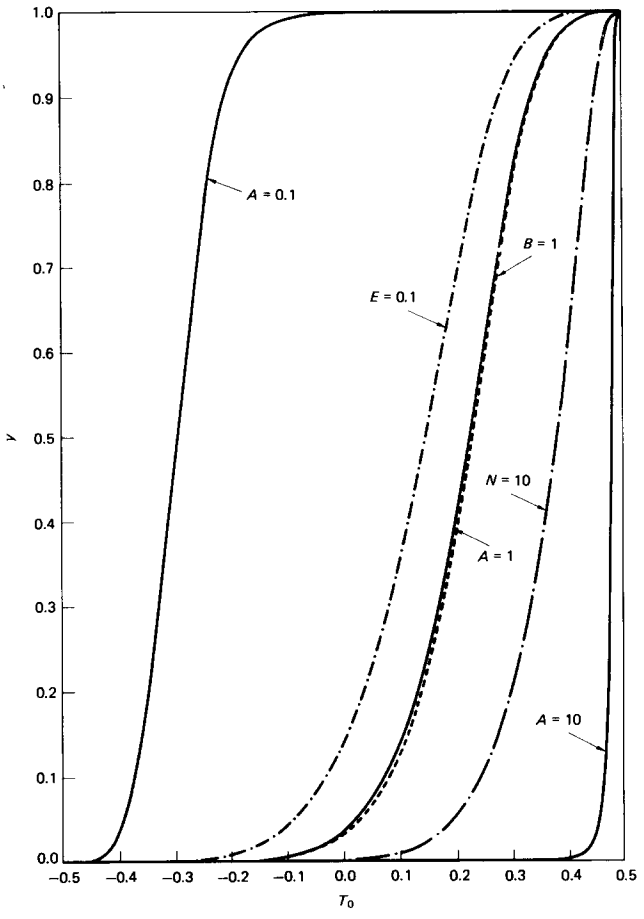

Figure 5 The wall temperature distribution for representative values of the parameters *A, B, E* and *N*. The notation for the lines is identical to that used in Fig 2

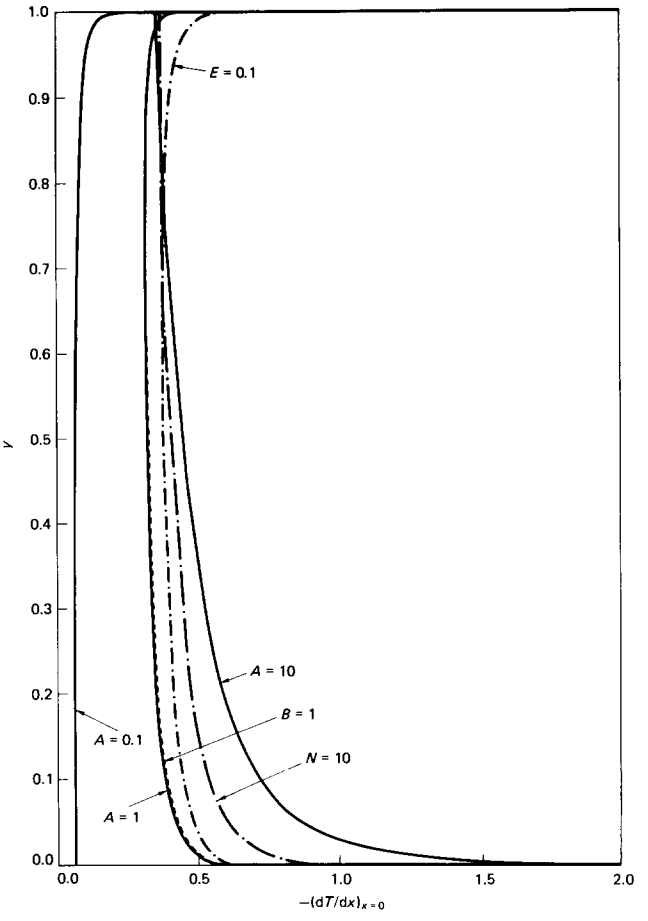

Figure 6 The wall heat flux distribution. The notation of the lines is identical to that used in Fig 2

Figs 5 and 6 depict the variation of the wall temperature and the wall heat flux with altitude for different values of the problem parameters. The wall temperature increases with height in an approximately linear manner in all cases. Near the two ends of the wall the wall temperature departs from its linear distribution and assumes the value of the reservoir temperatures (Fig 5). Increasing A has two main effects: (a) it yields a more uniform wall temperature distribution, and (b) it results in a temperature increase at all altitudes. The trend shown in Fig 5 implies that as a A becomes increasingly large the wall temperature approaches the temperature of the saturation reservoir. The effect of parameters B, E and N on the wall temperature distribution appears to be similar, although weaker, to the effect of A. Parameter B in particular has a minimal impact on the wall temperature distribution. With reference to the heat flux distribution at the interface (Fig 6) small values of A yield a practically constant heat flux along most of the interface. In addition, decreasing A suppresses the heat flux through the wall. Decreasing E as well as increasing N or B enhances the local heat flux. Parameter B appears to be again the least important.

A summary of useful results determining the dependence of the overall heat transfer through the wall on the dimensionless groups A, B, E and N is reported in Fig 7 and in Table 1 with the help of the conduction-referenced Nusselt number defined as

$$Nu \equiv \frac{Q}{k(T_s - T_c)} \tag{19}$$

where Q is the total heat flux through the wall obtained by integrating numerically the local heat flux over the entire wall height, and k is the porous medium effective thermal conductivity on the natural convection side. As shown in Fig 6, the local heat flux is singular at $y = 0, 1$. However, the overall

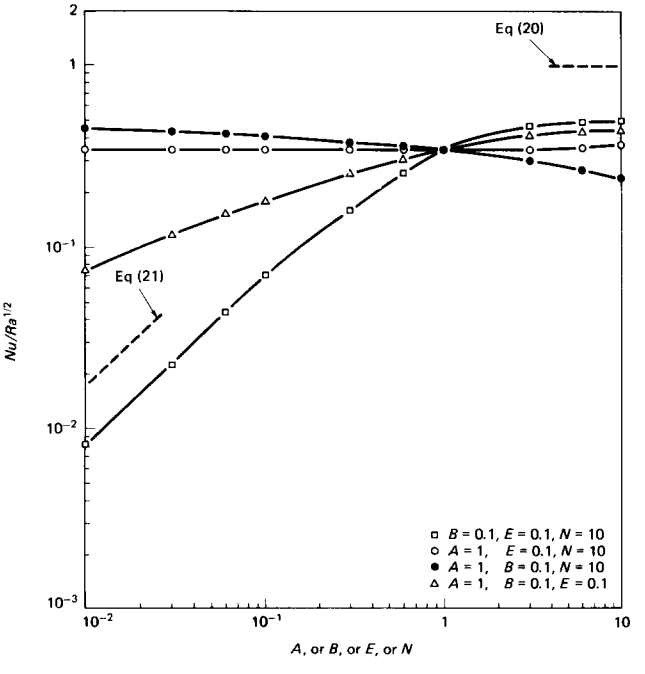

Figure 7 Summary of heat transfer results documenting the effect of parameters *A, B, E* and *N* on the overall heat flux

Table 1 Summary of heat transfer results

A	B	E	N	δ at $y=0$	$Nu\,Ra^{-1/2}$
10	0.1	1	1	0.555	0.4986
6	0.1	1	1	0.663	0.4917
3	0.1	1	1	0.838	0.4598
1	0.1	1	1	1.16	0.3423
0.6	0.1	1	1	1.301	0.2674
0.3	0.1	1	1	1.4565	0.1716
0.1	0.1	1	1	1.61	0.0709
0.06	0.1	1	1	1.65	0.0448
0.03	0.1	1	1	1.6865	0.0235
0.01	0.1	1	1	1.717	0.0082
1	10	1	1	0.909	0.3620
1	6	1	1	0.9765	0.3560
1	3	1	1	1.05	0.3505
1	1	1	1	1.119	0.3451
1	0.6	1	1	1.137	0.3444
1	0.3	1	1	1.15	0.3428
1	0.1	1	1	1.16	0.3427
1	0.06	1	1	1.1625	0.3426
1	0.03	1	1	1.164	0.3424
1	0.01	1	1	1.165	0.3423
1	0.1	10	1	1.023	0.2533
1	0.1	6	1	1.057	0.2743
1	0.1	3	1	1.099	0.3012
1	0.1	1	1	1.16	0.3423
1	0.1	0.6	1	1.185	0.3598
1	0.1	0.3	1	1.215	0.3813
1	0.1	0.1	1	1.2525	0.4081
1	0.1	0.06	1	1.265	0.4182
1	0.1	0.03	1	1.2784	0.4284
1	0.1	0.01	1	1.295	0.4415
1	0.1	1	10	0.533	0.4350
1	0.1	1	6	0.588	0.4238
1	0.1	1	3	0.721	0.3990
1	0.1	1	1	1.16	0.3424
1	0.1	1	0.6	1.5	0.3099
1	0.1	1	0.3	2.16	0.2629
1	0.1	1	0.1	3.893	0.1892
1	0.1	1	0.06	5.12	0.1587
1	0.1	1	0.03	7.4	0.1219
1	0.1	1	0.01	13.2	0.0756

heat flux is finite. Similar behaviour of the heat flux integral is reported in Refs 9 and 11–13.

Examining Fig 7 reveals that if E, B and N are kept constant, increasing A enhances the overall heat transfer through the wall until a plateau is reached for large values of A. This plateau corresponds to the case where the wall temperature is constant and identical to the temperature of the condensation reservoir ($T_o=\frac{1}{2}$). This result is also supported by the wall temperature profiles in Fig 5. Similarly, in the limit of small A the wall temperature approaches the temperature of the natural convection reservoir ($T_o=-\frac{1}{2}$). To check the correctness of the above statements further, we repeated the analysis in both limiting cases, namely large values of A and small values of A, by keeping the wall temperature constant in each case: $T_o=\frac{1}{2}$ and $T_o=-\frac{1}{2}$, respectively. Unfortunately, the complexity of the equations did not allow for analytical expressions for the Nusselt number[9,11,12] in either limit. However, it was observed that for $A<0.1$ and $A>10$ the constant wall temperature approximations estimate well the exact value of Nu. Since it was because of the algebraic complexity of the governing equations of the Brinkman-modified Darcy flow model that analytical expressions for Nu in the limits of large and small A were not possible to obtain, an attempt was made to obtain such expressions based on a simpler model for porous media flows, namely the Darcy model. The Darcy model does not account for macroscopic shear and does not satisfy the no-slip condition on the wall. The momentum equations for the Darcy model in each porous reservoir are obtained directly from the Brinkman-Darcy momentum equation by omitting the viscous shear term. Indeed, the simplicity of the Darcy model allows for the derivation of analytical expressions for the Nusselt number in the limits of high and low A

$$Nu=Ra^{1/2} \qquad \text{Darcy model } A\to\infty \tag{20}$$

$$Nu=2A\left(\frac{1+B}{2}\right)^{1/2}Ra^{1/2} \qquad \text{Darcy model } A\to 0 \tag{21}$$

As discussed by Bejan and Anderson[11], the similarity solution to the problem of natural convection from a constant-temperature wall in a Darcy porous medium reported by Cheng and Minkowycz[1] predicts that $Nu=0.888Ra^{1/2}$. This value of Nu falls within 12.6% of the Oseen-linearization result[20]. In Fig 7 it is shown that Refs 20 and 21 overpredict the overall heat transfer through the wall. This fact is explained as follows: since the Darcy flow model does not satisfy the no-slip condition on the wall, it allows for high velocities in the wall vicinity. As a result, an enhancement in the neat transfer to the fluid is induced, compared with the Brinkman-modified Darcy model.

The triangular symbols in Fig 7 correspond to the case $A=1$, $N=1$, $E=0.1$ and illustrate the effect of the subcooling parameter B on the overall heat transfer from the warm to the cold porous reservoir. Increasing B results in a slight increase in the overall heat transfer. However, it is clear that the dependence of Nu on the degree of subcooling in the condensation film is minimal.

The effect of parameter E on Nu for $A=1$, $B=0.1$, $N=1$ is reported in Fig 7 with the help of the square symbols. Increasing E causes a decrease in the value of the group $NuRa^{-1/2}$. Examining the definition of E shows that if Da is fixed, increasing E is equivalent to increasing Ra. An increase in Ra should cause an increase in the overall heat transfer through the wall (Nu). Making use of the values of Nu in Table 1 and Fig 7 we can easily prove that this is, in fact, true. However, the dependence of Nu on Ra is weaker than $Ra^{-1/2}$ which explains the decrease of the group $NuRa^{-1/2}$ with increasing E.

The dependence of Nu on the last parameter of interest, N, can be explained along the arguments used above in relation to parameter E. As the black circles in Fig 7 indicate, increasing N causes an increase in the value of the gorup $NuRa^{-1/2}$. According to the definition of N, if Da is held fixed, increasing N corresponds to decreasing Ra_f. Decreasing Ra_f, on the other hand, should yield a decrease in the value of Nu. However, examining the definition of A proves that for A to remain constant, decreasing Ra_f needs to be accompanied by an equivalent decrease in Ra. As mentioned above in the discussion pertinent to the effect of parameter E, the dependence of Nu on Ra is weaker than $Ra^{1/2}$. As a result, decreasing Ra (or increasing N) increases the value of the group $NuRa^{-1/2}$.

Partition with finite thermal resistance

In this section we relax the assumption that the thermal resistance of the wall separating the two porous reservoirs is negligible. The fact that the wall thickness is much smaller than the wall height ($L/H\to 0$) justifies the adoption of a one-dimensional conduction model to describe the heat transfer phenomenon within the wall. Based on the above, the temperature distribution in the wall varies linearly with x and assumes values between T_{oR} on the wall side facing the natural convection reservoir and T_{oL} on the wall side facing the condensation reservoir. Both T_{oL} and T_{oR} are altitude-dependent. In addition, at any given altitude the heat flux leaving the condensation (warm) space through the wall should equal the heat flux entering the natural convection (cold) space.

$$k_f\left(\frac{\partial\hat{T}}{\partial\hat{x}}\right)_{\hat{x}=0}=k\left(\frac{\partial T^*}{\partial x^*}\right)_{x^*=L}=k_w\frac{\partial T_o}{\partial x^*} \tag{22}$$

A relation between T_{oL} and T_{oR} can be obtained by using the

above heat flux continuity condition at either side of the wall. For algebraic simplicity we choose the condensation side. The relation between T_{oL} and T_{oR} then reads

$$T_{oL}=\frac{T_{oR}^{\delta'}+0.5w}{\delta'+w} \tag{23}$$

where

$$w=\frac{k_f}{k_w}\frac{L}{H}Ra_f^{1/2} \tag{24}$$

is the wall thermal resistance parameter. The nondimensionalization of Eq (23) was carried out on the basis of the previous definitions. It is worth noting (Eq (23)) that as the thermal resistance parameter decreases, the wall temperature on the side facing the condensation reservoir approaches the wall temperature on the side facing the natural convection reservoir.

The heat flux continuity matching condition at the wall needs to be rederived to take into account the temperature drop within the wall. The new matching condition is

$$A\frac{T_{oL}-\frac{1}{2}}{T_{oR}+\frac{1}{2}}=\frac{\delta'}{4mE}(1-4m^2E) \tag{25}$$

Lastly, the wall temperature T_o needs to be replaced by T_{oL} and by T_{oR} wherever appropriate for this part of the study. The remainder of the problem formulation remains unchanged. The solution methodology is identical to that used in the previous sections where the wall thermal resistance was neglected, taking into account the fact that T_{oL} and T_{oR} are related via Eq (24). The main results of the numerical solution are reported in Figs 8–10 and in Table 2. Increasing values of the thermal resistance parameter increase the wall temperature on the condensation side, Fig 8(a), and decrease the wall temperature on the natural convection side, Fig 8(b), at all altitudes. This result makes sense physically since large values of the wall thermal resistance parameter imply minimal thermal communication between the warm and the cold porous spaces. With the help of Fig 8, the following trend is verified: as the value of w becomes very large ($w\rightarrow\infty$) the wall temperature along the left side and the right side becomes equal to that of the respective porous reservoir.

The effect of the thermal resistance parameter on the wall local heat flux is depicted in Fig 9. Clearly, increasing w decreases the heat flux at all altitudes. The final illustration of this study, Fig 10, shows the impact of w on the value of Nu. Increasing w reduces the overall heat flux and, hence, the value of Nu. The dependence of Nu on w becomes less pronounced as w increases and becomes weak for w greater than approximately 6.

Conclusions

A theoretical investigation focusing on the interaction between film condensation and boundary layer natural convection in a porous material is reported. The natural convection flow was directed upward along one side of a vertical wall embedded in the porous medium. The condensation film was directed downward along the other side of the same wall. The two heat transfer phenomena, namely natural convection and film condensation, communicated thermally through the wall. The Brinkman-modified Darcy model was used to describe the flow in the porous medium on both sides of the wall. This model satisfies the no-slip condition on a solid boundary and accounts for friction induced by macroscopic shear. As such, the Brinkman-Darcy model is believed to be appropriate for flows in the neighbourhood of solid boundaries of the type encountered in this study.

The main results reported in this paper shed light on the variation of the wall temperature, the wall heat flux, the condensation film thickness and the natural convection boundary layer thickness with altitude. Representative results for the velocity and the temperature profiles in the horizontal

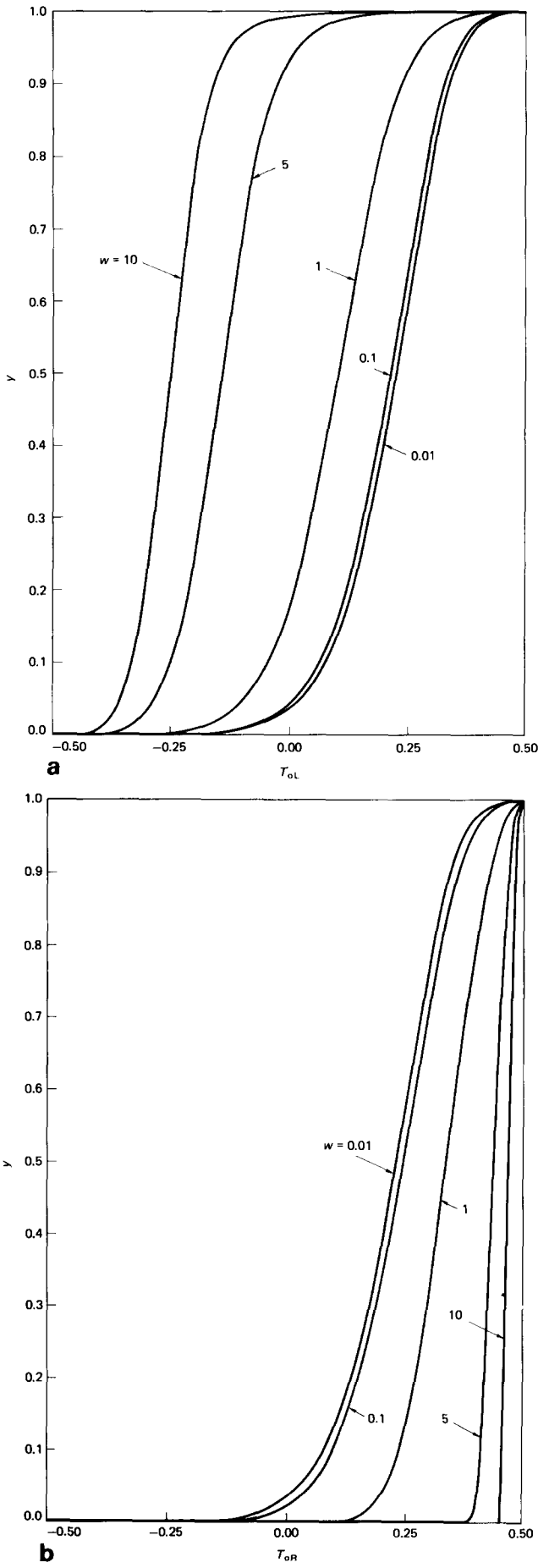

Figure 8 The effect of the thermal resistance parameter w on the wall temperature for $A=1$, $B=0.1$, $E=1$ and $N=1$: (a) side facing the condensation space; (b) side facing the natural convection space

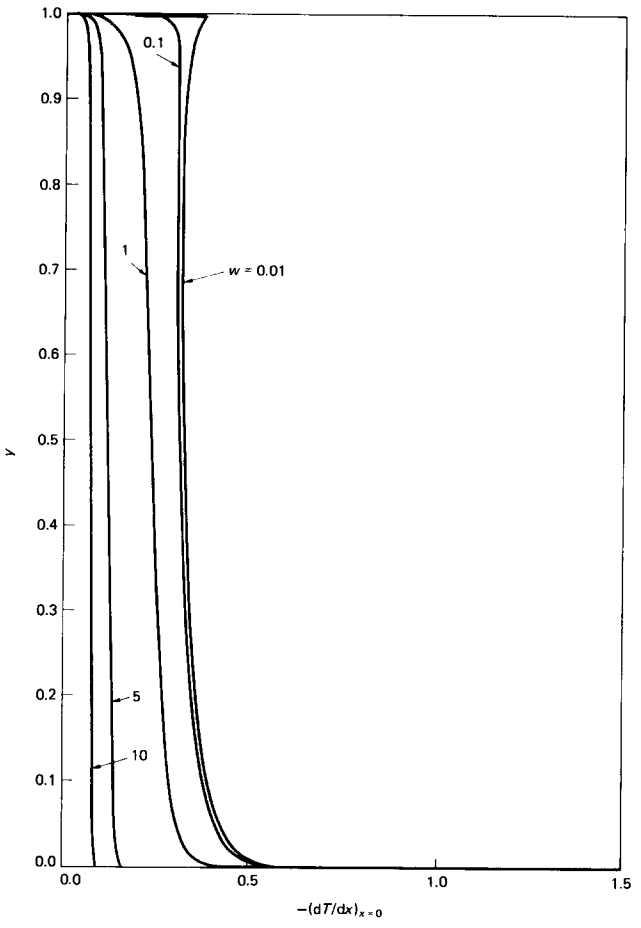

Figure 9 The effect of the thermal resistance parameter w on the wall heat flux distribution for $A=1$, $B=0.1$, $N=1$ and $E=1$

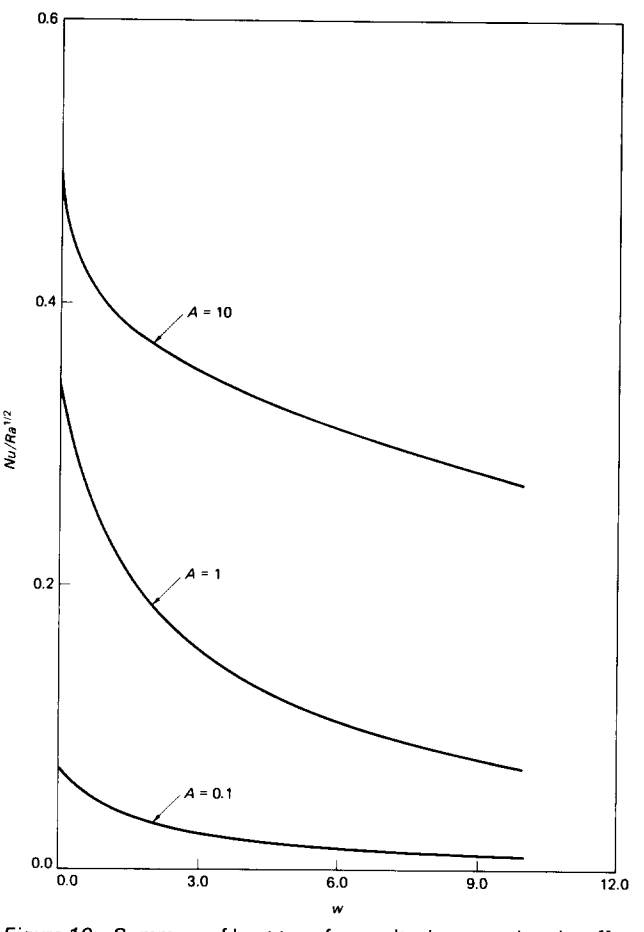

Figure 10 Summary of heat transfer results documenting the effect of the thermal resistance parameter w on the overall heat flux through the wall for $B=0.1$, $N=1$, $E=1$

direction within the two counterflowing layers are also reported. Finally, the dependence of the main heat and fluid flow characteristics of the problem on four dimensionless parameters A, B, E and N is thoroughly documented. It appears that parameter B had only a marginal effect on the phenomenon under investigation. In the other extreme, parameter A, which measures the heat transfer effectiveness of the condensation film relative to the natural convection boundary layer in the porous medium, had a paramount effect on the results. It was proved that large values of A correspond to the case of natural convection from an isothermal wall at T_s. Similarly, small values of A are relevant to film condensation from an isothermal wall at T_c. Asymptotic analytical expressions for the overall heat transfer through the wall for small and for large values of A based on the Darcy flow model (Eqs (21) and (22)) are also reported in this study. As expected, these expressions overpredict the overall heat transfer through the wall compared with the findings of the Brinkman-Darcy model. (Note that the Darcy model does not satisfy the no-slip condition on the wall.) However, Eqs (21) and (22) are in qualitative agreement with the numerical results. For the majority of values of parameters A, B, N and E examined in this study, the wall temperature exhibited an almost linear variation with altitude. The wall heat flux dependence on altitude was relatively weak except near the two ends of the wall.

In the last part of the study, the thermal resistance of the wall was taken into account. The effect of the thermal resistance on the results was illustrated with the help of the thermal resistance parameter w. It was found that increasing the thermal resistance parameter (ie limiting the thermal communication between the two porous reservoirs) increases the wall temperature on the condensation side, decreases the wall temperature on the natural convection side and reduces the heat transfer from the condensation to the natural convection porous space.

Table 2 The effect of the thermal resistance parameter on the overall heat transfer ($B=0.1$, $E=1$, $N=1$)

A	W	δ at $y=0$	$Nu/Ra^{1/2}$
0.1	0.0	1.6100	0.0709
0.1	0.01	1.6050	0.0704
0.1	0.1	1.5650	0.0668
0.1	0.2	1.5250	0.0632
0.1	0.4	1.4542	0.0571
0.1	1	1.2885	0.0437
0.1	2	1.1125	0.0311
0.1	4	0.9180	0.0194
0.1	5	0.8560	0.0162
0.1	7	0.7690	0.0123
0.1	10	0.6830	0.0090
1	0.0	1.160	0.3424
1	0.01	1.1570	0.3403
1	0.1	1.135	0.3252
1	0.2	1.1123	0.3099
1	0.4	1.073	0.2844
1	1.0	0.990	0.2338
1	2	0.8990	0.1838
1	4	0.7875	0.1307
1	5	0.7490	0.1146
1	7	0.690	0.0920
1	10	0.6270	0.0710
10	0.0	0.5555	0.4977
10	0.01	0.5546	0.4949
10	0.1	0.5451	0.470
10	0.2	0.5370	0.4510
10	0.4	0.5270	0.4292
10	1	0.5118	0.3983
10	2	0.4984	0.3717
10	4	0.4808	0.3371
10	5	0.4736	0.3233
10	7	0.4610	0.2998
10	10	0.4448	0.2710

Acknowledgement

Financial support for this research provided by NSF through grant ENG-8451144 is greatly appreciated.

References

1 Cheng, P. and Minkowycz, W. J. Free convection about a vertical flat plate embedded in a porous medium with application to heat transfer from a dike. *J. Geophys. Res.* 1977, **82**, 2040–2044
2 Bejan, A. and Poulikakos, D. The non-Darcy regime for vertical boundary layer natural convection in a porous medium. *Int. J. Heat Mass Transfer* 1984, **27**, 717–722
3 Plumb, D. A. and Huenefled, J. C. Non-Darcy natural convection from heated surfaces in saturated porous media. *Int. J. Heat Mass Transfer* 1981, **24**, 765–768
4 Hsu, C. T. and Cheng, P. The Brinkman model for natural convection about a semi-infinite vertical flat plate in a porous medium. *Int. J. Heat Mass Transfer* 1985, **28**, 683–697
5 Evans, G. E. and Plumb, O. A. Natural convection from a vertical isothermal surface embedded in a saturated porous medium. In Proceedings of the AIAA-ASME Thermophysics and Heat Transfer Conference, Paper No 78-HT-55, 1978
6 Cheng, P. Condensation along an inclined surface in a porous medium. *Int. J. Heat Mass Transfer* 1981, **14**, 983–990
7 Parmentier, E. M. Two-phase natural convection adjacent to a vertical heated surface in a permeable medium. *Int. J. Heat Mass Transfer* 1979, **27**, 849–855
8 Lock, G. S. H. and Ko, R. S. Coupling through a wall between two free convective systems. *Int. J. Heat Mass Transfer* 1973, **16**, 2087–2096
9 Anderson, R. and Bejan, A. Natural convection on both sides of a vertical wall separating fluids at different temperatures. *J. Heat Transfer* 1980, **102**, 630–635
10 Sparrow, E. M. and Prakash, C. Interaction between internal natural convection in an enclosure and an external natural convection boundary layer flow. *Int. J. Heat Mass Transfer* 1981, **24**, 875–907
11 Bejan, A. and Anderson, R. Natural convection at the interface between a vertical porous layer and an open space. *J. Heat Transfer* 1983, **105**, 124–129
12 Bejan, A. and Anderson, R. Heat transfer across a vertical impermeable partition embedded in porous medium. *Int. J. Heat Mass Transfer* 1981, **24**, 1237–1245
13 Gill, A. E. The boundary layer regime for convection in a rectangular cavity. *J. Fluid Mech.* 1966, **26**, 515–536
14 Rohsenow, W. M. Heat transfer and temperature distribution in laminar film condensation. *J. Heat Transfer* 1956, **78**, 1645–1648
15 Rohsenow, W. M., Hartnett, J. P. and Ganic, E. (eds) *Heat Transfer Fundamentals*, 2nd Edn, McGraw-Hill, 1985
16 Cheng, P. Heat transfer in geothermal systems. *Advances in Heat Transfer* 1979 **14**, 1–105
17 Brinkman, H. C. On the permeability of media consisting of closely packed porous particles. *Appl. Sci. Res., Sect. A.* 1947, **1**, 27–34
18 Vafai, K. Convective flow and heat transfer in variable porosity. *J. Fluid Mech.* 1984, **147**, 233–259
19 Poulikakos, D. and Bejan, A. Natural convection in vertically and horizontally layered porous media heated from the side. *Int. J. Heat Mass Transfer* 1983, **26**, 1805–1814
20 Tong, T. W. and Subramanian, E. A boundary layer analysis for natural convection in vertical porous enclosures—use of the Brinkman-extended Darcy model. *Int. J. Heat Mass Transfer* 1985, **28**, 563–571
21 Nield, D. A. The boundary correction of the Rayleigh–Darcy problem: limitations of the Brinkman equation. *J. Fluid Mech.* 1983, **128**, 37–46
22 Somerton, C. W. and Catton, I. On the thermal instability of superposed porous and fluid layers. *J. Heat Transfer*, 1982, **104**, 160–165
23 Bejan, A. *Convection Heat Transfer*, John Wiley and Sons, New York, 1984
24 Vovos, A. Natural Convection and Film Condensation in a Brinkman Porous Medium Coupled through a Vertical Impermeable Boundary. MS Thesis, University of Illinois at Chicago, 1985
25 Carnahan, B., Luther, L. A. and Wilkes, J. O. *Applied Numerical Methods*, John Wiley and Sons, New York, 1969
26 Ferziger, J. H. *Numerical Methods for Engineering Applications*, John Wiley and Sons, New York, 1981

Book review

Fundamentals of Hot Wire Anemometry

Charles G. Lomas

The author has set himself the task of providing a book which contains theoretical and practical information which would otherwise be acquired by researching the technical literature. This research is, of course, made easier by the perusal of instrumentation manuals and the house journals of companies which manufacture hot-wire instrumentation and most new users cannot avoid the need for extensive laboratory practice. At first sight, it is also facilitated by the publications of previous books which include material considered in this volume and particularly by that entitled 'Hot-Wire Aneometry' by A. E. Perry (Clarendon Press, 1982). The Cambridge volume does not reference that from Oxford.

The scope of Dr Lomas' book is different from that of Dr Perry although there is considerable overlap. It encompasses hot-film anemometry, as does the article by L. M. Fingerson and P. Freymuth (in Fluid Mechanics Measurements, ed. R. J. Goldstein, Springer-Verlag, 1983), considers some practical features of measurements in air, liquids and two-phase flows and discusses the measurement of vorticity, temperature, velocity-temperature correlations. The descriptions are helpful to a user and, though by no means exhaustive, provide a wide perspective of applications of hot-wires and films. There are, however, omissions which probably stem from the author's understandable lack of experience of all forms of the techniques which he describes. In the context of the probe-wire anemometry, for example, it would have been helpful to discuss the limitations imposed by size and by the inability to deal with high turbulence intensities.

The flavour is undoubtedly different from that of Dr Perry who provided a very detailed account of hot-wire anemometry, the transform equations and practical details essential to measurements of known accuracy. Here the emphasis tends to be more on breadth and the bringing together of known information to provide a valuable overview. The new user of hot-wire instrumentation will find the book of value, but it will not replace instrumentation manuals, the essential laboratory practice or the more detailed information provided by Dr Perry.

J. H. Whitelaw
Imperial College,
London, UK

Published price £35.00, Cambridge University Press, The Edinburgh Building, Shaftesbury Road, Cambridge CB2 2RU, UK, 211 pp.